AAS 11-588

OPTIMAL FEEDBACK GUIDANCE ALGORITHMS FOR PLANETARY LANDING AND ASTEROID INTERCEPT

Yanning Guo,[*] Matt Hawkins,[†] and Bong Wie[‡]

Optimal feedback guidance algorithms are investigated for planetary landing or asteroid intercept/rendezvous missions with a variety of terminal velocity constraints. This paper examines the well-known problems of constrained-terminal-velocity guidance (CTVG), free-terminal-velocity guidance (FTVG), and intercept-angle-control guidance (IACG), and presents some new results. It is shown that FTVG has a local optimal solution of the time-to-go for a certain set of initial conditions. It is also shown that a simple combination of the CTVG and FTVG algorithms can be employed for an intercept-angle control problem. Some inherent relationships of these optimal feedback guidance algorithms with the classical proportional navigation guidance (PNG), augmented PNG, biased PNG, and the zero-effort-miss (ZEM) and zero-effort-velocity (ZEV) feedback guidance are also discussed.

INTRODUCTION

The probable threat to planet Earth from the impact of an asteroid has led to increased interest in studying techniques to intercept and/or rendezvous with asteroids. In addition to responding to a threatening asteroid, scientific missions to visit asteroids, such as NASA's successful Deep Impact mission, will continue to drive interest in studying asteroid intercept and rendezvous. There is continued interest in landing on moons and planets with restrictions on the terminal velocity. This paper investigates optimal feedback guidance laws applied to the planetary landing and asteroid intercept problems.

Recent research on planetary landing has looked at optimal guidance laws with variable weighting on the mission time, but without explicitly considering constraints against subsurface travel.[1] Convex optimization has been used for open-loop control of a lander, taking into consideration physical constraints including no subsurface travel, as well as constraints on glide slope and minimum thrust level.[2] These results were extended to find the "best" trajectory when no feasible trajectory to the target exists.[3] The effects of guidance laws through all stages from entry to landing have been examined.[4]

[*] Ph.D. Candidate, Department of Control Science and Engineering, Harbin Institute of Technology, Main Building, Room 606, Harbin, Heilongjiang 150001. Currently, a visiting student at Asteroid Deflection Research Center, Iowa State University.
[†] Ph.D. Candidate, Department of Aerospace Engineering, Iowa State University, 2271 Howe Hall, Room 2348, Ames, IA 50011-2271.
[‡] Vance Coffman Endowed Chair Professor, Asteroid Deflection Research Center, Department of Aerospace Engineering, 2271 Howe Hall, Room 2355, Ames, IA 50011-2271.

In this paper, classical optimal feedback guidance theory is used, especially as it pertains to the design of spacecraft guidance algorithms.[5, 6] Classical proportional navigation and many related guidance schemes are considered.[7]

Optimal guidance laws based on the zero-effort-miss (ZEM) and zero-effort-velocity (ZEV) can command a spacecraft to a desired state, including both position and velocity, at the desired time. These laws can be made robust against disturbances using sliding-mode control.[8, 9]

Much work has been done on the problem of commanding intercept at a specified impact angle. Some of the earliest work led to guidance laws with strict limits on initial conditions.[10] Since then, a number of different laws with different advantages have been proposed. Various guidance laws exist that do not require the time-to-go,[11] that allow for significant target maneuvers,[12] and that can be used during hypersonic flight.[13] Linear-quadratic control laws have been derived,[14] as well as laws based on classical proportional navigation.[15] Guidance laws have been derived to follow a circular path to the target,[16] and to establish the desired end-of-mission geometry early on.[17] Many more impact-angle guidance concepts have also been studied in the literature.

The problem of intercepting a small solar system body at high velocities has been studied. NASA's Deep Impact mission successfully encountered comet Tempel 1.[18] Guidance algorithms to hit small, faint near-Earth objects (NEOs) have been tested with high-fidelity simulation software.[19, 20] Recently, a range of impact missions, from hypervelocity (10 km/s) impact to low speed (100 m/s) intercept with requirements on the final impact angle have also been investigated.[21, 22]

This paper is focused on the application of optimal feedback control algorithms for a variety of planetary or asteroid proximity operations, including asteroid rendezvous, soft landing, intercept, and intercept with impact angle control. Beginning with the general dynamic equations of motion, the constrained-terminal-velocity guidance (CTVG) algorithm and the free-terminal-velocity guidance (FTVG) algorithm are first described.

Computation methods to determine the time-to-go for these guidance laws are given. Connections are shown between these algorithms and various commonly used methods, including classical proportional navigation guidance (PNG) and augmented PNG, biased PNG, and optimal feedback control in terms of zero-effort-miss (ZEM) and zero-effort-velocity (ZEV). For a case with a terminal velocity vector pointing requirement, an intercept-angle-control guidance (IACG) algorithm is shown as a simple combination of the CTVG and FTVG algorithms along directions orthogonal to and parallel to the specified terminal velocity vector direction, respectively. Finally, numerical simulations are performed to demonstrate the validity and effectiveness of these algorithms.

Before continuing, a note on terminology is in order. In missile guidance, the impact angle is usually defined in terms of the inertial reference frame being used. The geometry of the target is not considered. For asteroid intercept, the angle of impact in the inertial frame is important for mission planning and operations. However, the angle that the spacecraft makes with the local horizontal of the asteroid's surface at impact is also important, whether for a subsurface penetrator or for pointing instruments. When considering the impact at the asteroid's surface, this angle is the impact angle, and the angle in inertial coordinates is called the approach (or intercept) angle. Because impact angle is common in missile guidance literature, and in this paper the local impact angle is not considered, the terms impact angle and approach angle will be used interchangeably.

EQUATIONS OF MOTION

The trajectory equations of motion of a spacecraft are described by

$$\dot{\mathbf{r}} = \mathbf{v} \tag{1}$$

$$\dot{\mathbf{v}} = \mathbf{g} + \mathbf{a} \tag{2}$$

$$\mathbf{a} = \frac{\mathbf{T}}{m} \tag{3}$$

where **r** and **v** are the position and velocity vectors; **a** is the control acceleration provided by the thrusting force **T**; m is the spacecraft mass; and **g** denotes the gravitational acceleration acting on the spacecraft. In general, we have **g** = **g**(**r**, t). However, depending on the problem, the gravitational acceleration **g** can be assumed to be constant or negligible for practical applications.

The thrust magnitude T of a spacecraft engine is modeled as

$$T = |\mathbf{T}| = -\dot{m}c \tag{4}$$

where $\dot{m}$ is the negative mass flow rate and $c = I_{sp} g_o$ is the engine exhaust velocity. For a power-limited or a variable-specific-impulse engine,[23,24,25] the power required for a given thrust T is expressed as

$$P = \frac{1}{2}|\dot{m}|c^2 = \frac{1}{2}cT \le P_{\max} \tag{5}$$

where $P_{\max}$ is the maximum power available to the engine. For many practical applications, the engine exhaust velocity is often assumed to be constant and the thrust magnitude is then assumed as

$$0 \le T \le T_{\max} \tag{6}$$

where $T_{\max}$ is the maximum thrust available.

OPTIMAL FEEDBACK GUIDANCE ALGORITHMS

Several optimal feedback guidance algorithms are described in this section for different terminal velocity requirements, including constrained terminal velocity, free terminal velocity, and terminal velocity pointing. Real-time calculation methods for determining the time-to-go are provided for practical implementation of these optimal feedback guidance algorithms.

Constrained-Terminal-Velocity Guidance (CTVG)

Consider a classical optimization problem with the following performance index

$$J = \frac{1}{2}\int_{t_0}^{t_f} \mathbf{a}^T \mathbf{a}\, dt \tag{7}$$

subject to Eqs. (1) through (3) and the following given boundary conditions:

$$\begin{aligned} &\mathbf{r}(t_0) = \mathbf{r}_0, \ \mathbf{r}(t_f) = \mathbf{r}_f \\ &\mathbf{v}(t_0) = \mathbf{v}_0, \ \mathbf{v}(t_f) = \mathbf{v}_f \end{aligned} \tag{8}$$

The Hamiltonian function is defined as

$$H = \frac{1}{2}\mathbf{a}^T\mathbf{a} + \mathbf{p}_r^T\mathbf{v} + \mathbf{p}_\mathrm{v}^T(\mathbf{g}+\mathbf{a}) \tag{9}$$

where $\mathbf{p}_r$ and $\mathbf{p}_\mathrm{v}$ are the costate vectors associated with the position and velocity vectors, respectively.

Assuming that $\mathbf{g}$ is a constant vector, especially for a typical planetary landing problem, we obtain the costate equations and the optimal control equation as

$$\dot{\mathbf{p}}_r = -\frac{\partial H}{\partial \mathbf{r}} = 0 \tag{10}$$

$$\dot{\mathbf{p}}_\mathrm{v} = -\frac{\partial H}{\partial \mathbf{v}} = -\mathbf{p}_r \tag{11}$$

$$\frac{\partial H}{\partial \mathbf{a}} = 0 \quad \Rightarrow \ \mathbf{a} = -\mathbf{p}_\mathrm{v} \tag{12}$$

Defining $t_{go} = t_f - t$ as the time-to-go before arriving at the terminal state, we obtain the solutions of the costate equations as

$$\mathbf{p}_r = \mathbf{p}_r(t_f) \tag{13}$$

$$\mathbf{p}_\mathrm{v} = t_{go}\mathbf{p}_r(t_f) + \mathbf{p}_\mathrm{v}(t_f) \tag{14}$$

The optimal control solution is then expressed as

$$\mathbf{a} = -t_{go}\mathbf{p}_r(t_f) - \mathbf{p}_\mathrm{v}(t_f) \tag{15}$$

and the states are expressed as

$$\mathbf{v} = \frac{t_{go}^2}{2}\mathbf{p}_r(t_f) + t_{go}\mathbf{p}_\mathrm{v}(t_f) - t_{go}\mathbf{g} + \mathbf{v}_f \tag{16}$$

$$\mathbf{r} = -\frac{t_{go}^3}{6}\mathbf{p}_r(t_f) - \frac{t_{go}^2}{2}\mathbf{p}_\mathrm{v}(t_f) + \frac{t_{go}^2}{2}\mathbf{g} - t_{go}\mathbf{v}_f + \mathbf{r}_f \tag{17}$$

Combining Eq. (16) and Eq. (17) leads to

$$\mathbf{p}_r(t_f) = \frac{6(\mathbf{v}+\mathbf{v}_f)}{t_{go}^2} + \frac{12(\mathbf{r}-\mathbf{r}_f)}{t_{go}^3} \tag{18}$$

$$\mathbf{p}_\mathrm{v}(t_f) = -\frac{2(\mathbf{v}+2\mathbf{v}_f)}{t_{go}} - \frac{6(\mathbf{r}-\mathbf{r}_f)}{t_{go}^2} + \mathbf{g} \tag{19}$$

Finally, the CTVG law with the specified $\mathbf{r}_f$, $\mathbf{v}_f$, and t_{go} is obtained as

$$\mathbf{a} = \frac{6\left[\mathbf{r}_f - (\mathbf{r}+t_{go}\mathbf{v})\right]}{t_{go}^2} - \frac{2(\mathbf{v}_f - \mathbf{v})}{t_{go}} - \mathbf{g} \tag{20}$$

or

$$\mathbf{a} = \frac{6\left[\mathbf{r}_f - \left(\mathbf{r} + t_{go}\mathbf{v}_f\right)\right]}{t_{go}^2} + \frac{4\left(\mathbf{v}_f - \mathbf{v}\right)}{t_{go}} - \mathbf{g} \tag{21}$$

For a soft landing problem with $\mathbf{v}_f = 0$, the CTVG law has the following well-known form

$$\mathbf{a} = \frac{6\left(\mathbf{r}_f - \mathbf{r}\right)}{t_{go}^2} - \frac{4\mathbf{v}}{t_{go}} - \mathbf{g} \tag{22}$$

While the CTVG law described by Eq. (20) or Eq. (22) assumes a uniform gravitational field (i.e., constant **g**), it can be extended to a case when **g** is only an explicit function of time, though this is rare in practice. By repeating the same derivation procedure, the optimal CTVG algorithm can be expressed as

$$\mathbf{a} = \frac{6\left[\mathbf{r}_f - \left(\mathbf{r} + t_{go}\mathbf{v}\right)\right]}{t_{go}^2} - \frac{2\left(\mathbf{v}_f - \mathbf{v}\right)}{t_{go}} + \frac{6\int_t^{t_f}\left(\tau - t\right)\mathbf{g}(\tau)d\tau}{t_{go}^2} - \frac{4\int_t^{t_f}\mathbf{g}(\tau)d\tau}{t_{go}} \tag{23}$$

Defining the zero-effort-miss (**ZEM**) and zero-effort-velocity (**ZEV**) as follows:[8,9]

$$\begin{aligned}
\mathbf{ZEV} &= \mathbf{v}_f - \left[\mathbf{v} + \int_t^{t_f}\mathbf{g}(\tau)d\tau\right] \\
\mathbf{ZEM} &= \mathbf{r}_f - \left[\mathbf{r} + t_{go}\mathbf{v} + \int_t^{t_f}\left(t_f - \tau\right)\mathbf{g}(\tau)d\tau\right] \\
&= \mathbf{r}_f - \left[\mathbf{r} + t_{go}\mathbf{v} + t_{go}\int_t^{t_f}\mathbf{g}(\tau)d\tau - \int_t^{t_f}\left(\tau - t\right)\mathbf{g}(\tau)d\tau\right]
\end{aligned} \tag{24}$$

we obtain the CTVG law of the form

$$\mathbf{a} = \frac{6}{t_{go}^2}\mathbf{ZEM} - \frac{2}{t_{go}}\mathbf{ZEV} \tag{25}$$

Computation of the time-to-go for CTVG

As can be noticed in Eqs. (20) and (21), the CTVG algorithm requires the final time (or the time of flight) be specified. However, when the time of flight is not specified, a method for computing the flight time is needed to minimize the control effort.

For a case with constant **g**, the transversality condition is given by

$$\begin{aligned}
\frac{\partial J^*}{\partial t_{go}} = \frac{\partial J^*}{\partial t_f} &= H = \text{constant on the optimal trajectory} \\
&= 0 \quad \text{when } t_f \text{ is free}
\end{aligned} \tag{26}$$

where J^* is the optimal value of the performance index. The Hamiltonian function of the form

$$H = -\frac{1}{2}\mathbf{a}^T\left(\mathbf{a} + 2\mathbf{g}\right) + \mathbf{p}_r^T\mathbf{v} \tag{27}$$

becomes

$$H = \frac{1}{t_{go}^4}\left[t_{go}^4 \left(\mathbf{g}^T\mathbf{g} + \Gamma \right) - 2t_{go}^2 \left(\mathbf{v}^T\mathbf{v} + \mathbf{v}_f^T\mathbf{v} + \mathbf{v}_f^T\mathbf{v}_f \right) + t_{go} 12 \left(\mathbf{r}_f - \mathbf{r} \right)^T \left(\mathbf{v} + \mathbf{v}_f \right) - 18 \left(\mathbf{r}_f - \mathbf{r} \right)^T \left(\mathbf{r}_f - \mathbf{r} \right) \right] \quad (28)$$

and Eq. (26) becomes

$$t_{go}^4 \mathbf{g}^T\mathbf{g} - 2t_{go}^2 \left(\mathbf{v}^T\mathbf{v} + \mathbf{v}_f^T\mathbf{v} + \mathbf{v}_f^T\mathbf{v}_f \right) + t_{go} 12 \left(\mathbf{r}_f - \mathbf{r} \right)^T \left(\mathbf{v} + \mathbf{v}_f \right) - 18 \left(\mathbf{r}_f - \mathbf{r} \right)^T \left(\mathbf{r}_f - \mathbf{r} \right) = 0 \quad (29)$$

which is to be used to determine the time-to-go.[1]

For a special case with negligible **g**, Eq. (29) becomes

$$t_{go}^2 \left(\mathbf{v}^T\mathbf{v} + \mathbf{v}_f^T\mathbf{v} + \mathbf{v}_f^T\mathbf{v}_f \right) - t_{go} 6 \left(\mathbf{r}_f - \mathbf{r} \right)^T \left(\mathbf{v} + \mathbf{v}_f \right) + 9 \left(\mathbf{r}_f - \mathbf{r} \right)^T \left(\mathbf{r}_f - \mathbf{r} \right) = 0 \quad (30)$$

and the time-to-go can be calculated as follows:

$$t_{go} = \begin{cases} \tau & ; \quad B^2 - 4AC > 0 \quad \text{and} \quad B < 0 \\ \text{no solution} & ; \quad \text{otherwise} \end{cases} \quad (31)$$

where

$$\tau = \frac{-B - \sqrt{B^2 - 4AC}}{2A}$$

$$A = \mathbf{v}^T\mathbf{v} + \mathbf{v}_f^T\mathbf{v} + \mathbf{v}_f^T\mathbf{v}_f \geq 0$$

$$B = -6 \left(\mathbf{r}_f - \mathbf{r} \right)^T \left(\mathbf{v} + \mathbf{v}_f \right)$$

$$C = 9 \left(\mathbf{r}_f - \mathbf{r} \right)^T \left(\mathbf{r}_f - \mathbf{r} \right) \geq 0$$

and τ is the smaller positive solution of Eq. (30) which leads to a local minimum of J^*. The other, larger solution of Eq. (30) corresponds to a local maximum of J^*, and J^* decreases monotonically with respect to t_{go} when it is greater than the larger solution. Note that for the "no-solution" condition, the partial derivative of J^* expressed in Eq. (26) is always negative, thus as t_{go} increases, the performance index decreases, or equivalently, less control effort is used.

CTVG under acceleration magnitude and flight time constraints

Consider a case when t_f is constrained as

$$t_1 \leq t_f \leq t_2 \quad (32)$$

where t_1 and t_2 denote the lower and upper bounds of t_f, respectively.

We can then determine the time-to-go using the following logic

$$t_{go} = \begin{cases} t_2 - t & ; \quad \textit{otherwise} \\ t_1 - t & ; \quad \tau < t_1 - t \\ \tau & ; \quad t_1 - t \leq \tau \leq t_2 - t \end{cases} \quad (33)$$

If the control thrust magnitude is constrained as

$$T = |\mathbf{T}| = m|\mathbf{a}| \leq T_{\max} \quad (34)$$

the CTVG algorithm has the following form

$$\mathbf{a} = \underset{T_{\max}/m}{\text{sat}}\left(\frac{6\left[\mathbf{r}_f - \left(\mathbf{r} + t_{go}\mathbf{v}\right)\right]}{t_{go}^2} - \frac{2\left(\mathbf{v}_f - \mathbf{v}\right)}{t_{go}} - \mathbf{g} \right) \tag{35}$$

where the normalized saturation function of a vector **x** is defined as

$$\underset{U}{\text{sat}}\left(\mathbf{x}\right) = \begin{cases} \mathbf{x} & \text{if} \quad |\mathbf{x}| \le U \\ \mathbf{x}\dfrac{U}{|\mathbf{x}|} & \text{if} \quad |\mathbf{x}| > U \end{cases} \tag{36}$$

where |**x**| depicts the two norm of a vector **x**.

Free-Terminal-Velocity Guidance (FTVG)

If the terminal velocity is unconstrained and **g** is a constant vector, we have $\mathbf{p}_v(t_f) = 0$ and

$$\mathbf{p}_{\mathrm{v}} = t_{go}\mathbf{p}_r(t_f) \tag{37}$$

$$\mathbf{a} = -\mathbf{p}_{\mathrm{v}} = -t_{go}\mathbf{p}_r(t_f) \tag{38}$$

$$\mathbf{v} = \frac{t_{go}^2}{2}\mathbf{p}_r(t_f) - t_{go}\mathbf{g} + \mathbf{v}_f \tag{39}$$

$$\mathbf{r} = -\frac{t_{go}^3}{6}\mathbf{p}_r(t_f) + \frac{t_{go}^2}{2}\mathbf{g} - t_{go}\mathbf{v}_f + \mathbf{r}_f \tag{40}$$

Combining these equations gives

$$\mathbf{p}_r(t_f) = -\frac{3}{t_{go}^3}\left(\mathbf{r}_f - \mathbf{r} - \mathbf{v}t_{go} - \frac{t_{go}^2}{2}\mathbf{g} \right) \tag{41}$$

$$\mathbf{v}_f = \frac{3}{2t_{go}}\left(\mathbf{r}_f - \mathbf{r}\right) - \frac{1}{2}\mathbf{v} + \frac{1}{4}t_{go}\mathbf{g} \tag{42}$$

Finally, the optimal FTVG acceleration command is obtained as

$$\mathbf{a} = \frac{3}{t_{go}^2}\left(\mathbf{r}_f - \mathbf{r}\right) - \frac{3}{t_{go}}\mathbf{v} - \frac{3}{2}\mathbf{g} \tag{43}$$

If **g** is only an explicit function of time, we have the optimal FTVG algorithm of the form

$$\mathbf{a} = \frac{3}{t_{go}^2}\left[\mathbf{r}_f - \mathbf{r} - t_{go}\mathbf{v} - t_{go}\int_t^{t_f} \mathbf{g}(\tau)d\tau + \int_t^{t_f} \left(\tau - t\right)\mathbf{g}(\tau)d\tau \right] = \frac{3}{t_{go}^2}\,\mathbf{ZEM} \tag{44}$$

Computation of time-to-go for FTVG

Similar to Eq. (29), we can find the following equation for computing the time-to-go:

$$t_{go}^4 \mathbf{g}^T\mathbf{g} - 4t_{go}^2\left[\mathbf{v}^T\mathbf{v} - \left(\mathbf{r}_f - \mathbf{r}\right)^T\mathbf{g}\right] + 16t_{go}\left(\mathbf{r}_f - \mathbf{r}\right)^T\mathbf{v} - 12\left(\mathbf{r}_f - \mathbf{r}\right)^T\left(\mathbf{r}_f - \mathbf{r}\right) = 0 \tag{45}$$

When $\mathbf{g} = 0$, this equation simply becomes

$$t_{go}^2\mathbf{v}^T\mathbf{v} - 4t_{go}\left(\mathbf{r}_f - \mathbf{r}\right)^T\mathbf{v} + 3\left(\mathbf{r}_f - \mathbf{r}\right)^T\left(\mathbf{r}_f - \mathbf{r}\right) = 0 \tag{46}$$

Defining θ as the angle between the vectors $\mathbf{v}$ and $\mathbf{r}_f - \mathbf{r}$, we can find the solution of Eq. (46)as

$$\tau = \frac{2\left|\mathbf{r}_f - \mathbf{r}\right|}{\left|\mathbf{v}\right|}\left(\cos\theta - \sqrt{\cos^2\theta - 3/4}\right) \;; \qquad \theta \in (-30°, 30°) \tag{47}$$

Note that there exists a finite solution for t_{go} only when $\theta \in (-30°, 30°)$.

Relationship with Proportion Navigational Guidance (*PNG*) *Logic*

Consider a two-dimensional problem with

$$\begin{aligned} \mathbf{r}_f - \mathbf{r} &= [x \quad y]^T \\ -\mathbf{v} &= [\dot{x} \quad \dot{y}]^T \end{aligned} \tag{48}$$

$$\lambda = \arctan\frac{y}{x} \tag{49}$$

where λ is the line-of-sight (LOS) angle between the spacecraft and the target. Let $R = |\mathbf{r}_f - \mathbf{r}|$ be the LOS distance between the spacecraft and target, then the closing velocity V_c and the time-to-go are obtained as

$$V_c = -\dot{R} \;; \qquad t_{go} = \frac{R}{V_c} \tag{50}$$

and the optimal FTVG algorithm becomes

$$\mathbf{a} = 3V_c\dot{\lambda}\begin{bmatrix} -\sin\lambda \\ \cos\lambda \end{bmatrix} - \frac{3}{2}\mathbf{g} \tag{51}$$

which is the so-called augmented PNG logic or PNG with gravity compensation,[7] with an effective navigation ratio of 3. The augmented PNG acceleration perpendicular to the LOS direction is often expressed as[7]

$$a = NV_c\dot{\lambda} - \frac{N}{2}g \tag{52}$$

where N is the effective navigation ratio and g is the component of $\mathbf{g}$ perpendicular to the line-of-sight direction.

A special case of straight line motion

For a special case with $\mathbf{g} = 0$ and $\theta = 0$ (i.e., the spacecraft is moving straight toward the target without any disturbance), the solutions of Eq. (46) are given as

$$\tau_1 = \frac{r_f - r}{\mathrm{v}}, \qquad \tau_2 = \frac{3\left(r_f - r\right)}{\mathrm{v}} \tag{53}$$

The terminal velocities are obtained using Eq. (42) as

$$\mathrm{v}_{\tau 1} = \mathrm{v}, \qquad \mathrm{v}_{\tau 2} = 0 \tag{54}$$

This result suggests that depending on a chosen final time, which can be larger or smaller than τ_2, either a positive or a negative terminal velocity can be obtained. This situation will be further discussed in the next section on intercept-angle-control guidance.

FTVG under acceleration magnitude and flight time constraints

The FTVG algorithm accommodating the constraints on control thrust magnitude and flight time can be expressed as

$$\mathbf{a} = \underset{T_{\max}/m}{\mathrm{sat}}\left(\frac{3}{t_{go}^2}\left(\mathbf{r}_f - \mathbf{r}\right) - \frac{3}{t_{go}}\mathbf{v} - \frac{3}{2}\mathbf{g} \right) \tag{55}$$

Intercept-Angle-Control Guidance (IACG)

Consider a guidance problem that has the intercept-time and intercept-angle constraints.[10-17] For this case, the terminal velocity vector has a specified direction but with free magnitude, and we may consider a simple combination of the CTVG and FTVG logic.

Let $\mathbf{e}_1$ be the unit vector in the desired final velocity direction, and ($\mathbf{e}_2$, $\mathbf{e}_3$) be the two orthogonal vectors perpendicular to $\mathbf{e}_1$. Then the acceleration vector is expressed as

$$\mathbf{a} \coloneqq a_1\mathbf{e}_1 + a_2\mathbf{e}_2 + a_3\mathbf{e}_3 \tag{56}$$

Consequently, the performance index described by Eq. (7) simply becomes

$$J = \frac{1}{2}\int_{t_0}^{t_f}\left(a_1^2 + a_2^2 + a_3^2\right)dt \tag{57}$$

Similar to the acceleration vector expressed in terms of the new basis vectors $(\mathbf{e}_1, \mathbf{e}_2, \mathbf{e}_3)$, let the position, velocity, and gravity vectors be expressed as

$$\mathbf{r} \coloneqq r_1\mathbf{e}_1 + r_2\mathbf{e}_2 + r_3\mathbf{e}_3; \quad \mathbf{v} \coloneqq \mathrm{v}_1\mathbf{e}_1 + \mathrm{v}_2\mathbf{e}_2 + \mathrm{v}_3\mathbf{e}_3; \quad \mathbf{g} \coloneqq g_1\mathbf{e}_1 + g_2\mathbf{e}_2 + g_3\mathbf{e}_3 \tag{58}$$

Assuming that v_1 is free and (v_2, v_3) are specified, we propose a simple IACG algorithm that combines the CTVG and FTVG, as follows:

$$\mathbf{a} \coloneqq \left(\frac{3\left(r_{f1} - r_1\right)}{t_{go}^2} - \frac{3\mathrm{v}_1}{t_{go}} - \frac{3g_1}{2} \right)\mathbf{e}_1 + \left(\frac{6\left(r_{f2} - r_2\right)}{t_{go}^2} - \frac{4\mathrm{v}_2}{t_{go}} - g_2 \right)\mathbf{e}_2 + \left(\frac{6\left(r_{f3} - r_3\right)}{t_{go}^2} - \frac{4\mathrm{v}_3}{t_{go}} - g_3 \right)\mathbf{e}_3 \tag{59}$$

This proposed IACG algorithm can also be represented as

$$\mathbf{a} = \left(3\mathbf{e}_1\mathbf{e}_1^T + 6\mathbf{e}_2\mathbf{e}_2^T + 6\mathbf{e}_3\mathbf{e}_3^T\right)\frac{\mathbf{r}_f - \mathbf{r}}{t_{go}^2} - \left(3\mathbf{e}_1\mathbf{e}_1^T + 4\mathbf{e}_2\mathbf{e}_2^T + 4\mathbf{e}_3\mathbf{e}_3^T\right)\frac{\mathbf{v}}{t_{go}} - \left(\frac{3}{2}\mathbf{e}_1\mathbf{e}_1^T + \mathbf{e}_2\mathbf{e}_2^T + \mathbf{e}_3\mathbf{e}_3^T\right)\mathbf{g} \tag{60}$$

All vectors in Eq. (60) can be expressed in any reference frame, including the inertial reference frame. Note that one drawback of the proposed, simple IACG logic is that the terminal velocity vector is constrained to be only parallel to a specified direction (i.e., v_1 is free). Hence, in some cases the terminal velocity may be opposite the desired direction. However, as long as the

spacecraft is initially moving toward the target position along the given direction with $(r_{f1} - r_1)\, v_1 > 0$ and with a properly chosen time-to-go, as discussed in the preceding sections, the IACG algorithm can also deal with the prescribed impact angle direction. Otherwise, when $(r_{f1} - r_1)\, v_1 \leq 0$, the CTVG logic must be used to work together with IACG to fulfill the correct directional impact requirement.

Relationship with PNG Algorithm with Intercept Angle Constraint

For the case with a two-dimensional, small-angle approximation, the proposed IACG algorithm becomes the augmented or biased PNG with commanded line-of-sight angle[7]

$$a = 4V_c\dot{\lambda} + 2V_c\frac{\lambda - \lambda_f}{t_{go}} - g \tag{61}$$

where λ and λ_f denote the current and commanded line-of-sight angle, respectively and t_{go} is estimated as R/V_c.

NUMERICAL SIMULATION EXAMPLES

In this section, simulation study results of three illustrative cases are discussed in order to examine the validity and effectiveness of the three optimal algorithms described in this paper. For Case 1, the CTVG algorithm is applied to a Mars pinpoint landing problem considered in Ref. 2. In Case 2, FTVG is applied to an asteroid intercept problem and compared to PNG. The existence of a local minimum solution is also validated by numerical results. In Case 3, several tests are carried out to evaluate the effectiveness of the proposed IACG algorithm, comparing with the PNG algorithm with impact angle constraint.

Throughout the numerical simulation studies, we assumed that the system states can be measured with no error even though these feedback controllers possess good performance robustness. A generic spacecraft model from Ref. 2 is used for these three test cases. The initial mass of the spacecraft is 1905 kg and the engine exhaust velocity is assumed as 1.964 km/s ($1/c = 5.09\times10^{-4}$ s/m). A 4th order Runge-Kutta numerical integrator with an interval time of 0.1 s is used. During the last two integration steps, t_{go} is held at 0.2 s to avoid any numerical singularity problem.

Case 1: CTVG Applied to Mars Pinpoint Landing Problem (Ref. 2)

In Ref. 2, the maximum control force from the thrusters is assumed as 16.573 kN, of which only 80% is used for control, for a conservative solution. The pinpoint landing mission starts with initial conditions of $\mathbf{r}_0 = (2, 1.5, 0)$ km, $\mathbf{v}_0 = (100, -75, 0)$ m/s, and the landing site is assumed to be located at the origin of the (x, y, z) coordinates, i.e., $\mathbf{r}_f = (0, 0, 0)$ m. The terminal velocity is specified as zero for soft landing. A uniform gravitational field of Mars is assumed as: $\mathbf{g} = (0, -3.7114, 0)$ m/s^2.

Simulation results using the CTVG algorithm for a Mars pinpoint landing problem are presented in Figures 1 through 3. The CTVG algorithm is only concerned with the boundary conditions at the beginning and the end of the mission and it has no consideration on any kind of constraints on the states. Consequently, there exists a possibility that for planetary landing, the spacecraft may hit the surface before landing at the desired site. This is illustrated as the "without an intermediate target" case in Figure 3. If an intermediate waypoint state is specified as a temporary target, the spacecraft can maneuver safely and a no-subsurface constraint or a glide slope constraint, as used in Ref. 2, can be enforced. The intermediate waypoint target was selected as $\mathbf{r} = (2, 0.35, 0)$ km, $\mathbf{v} = (-75, 0, 0)$ m/s at $t = 50$ s. This corresponds to a point directly beneath the

initial position with its velocity toward the target. There are many other alternative choices for the waypoint state, selection of which is an area for further study.

As shown in Figure 1, the spacecraft achieves both target points (intermediate and final) successfully with the control thrust force under a saturation constraint. Total flight time is t_f = 83 s. Figure 2 provides various plots, including the time histories of ΔV, performance index, mass consumption, and throttle level of the thrust. Figure 2 shows that 404.8 kg of propellant is consumed by this simple feedback CTVG algorithm, which is very close to the minimum value of 399.5 kg required by the off-line convex programming approach described in Ref. 2. It is also shown in Figure 2 that the actual thrust force is well-constrained under the chosen saturation constraint. However, note that the lower bound of the throttle level of thrust is not considered in this example. The effectiveness of the simple CTVG algorithm has been demonstrated for the precision planetary landing problem of Ref. 2; however, a further detailed evaluation study of this algorithm is needed, especially for optimal intermediate waypoint target selection.

Case 2: FTVG Applied to Asteroid Intercept Problem

For the purpose of concept illustration, it is assumed that any landmark point on the asteroid surface can be chosen as the final intercept location depending on the mission requirements, surface conditions, and the terminal-phase duration. The same spacecraft parameters employed for Case 1 are also used here. It is further assumed that $\mathbf{g} = (0, 0, 0)\ \text{m/s}^2$. The thrust magnitude constraint is not considered in order to validate the method of computing the local optimal time-to-go.

An intercept problem considered here is to maneuver the spacecraft from the given initial conditions of $\mathbf{r}_0 = (-2, 0.5, 0)$ km and $\mathbf{v}_0 = (70, 10, 0)$ m/s to the origin within the time range of 10 s to 100 s. Since the terminal velocity is assumed to be free, the FTVG algorithm is suitable for this case, and the flight time can be generated by the time-to-go Eqs. (33) and (47).

Figures 4 and 5 show the simulation results of the FTVG and PNG algorithms, respectively. It is shown that both algorithms work well for this test case. The PNG logic with an effective navigation ratio of 4 requires slightly larger acceleration and control thrust force. Performance comparisons between FTVG and PNG algorithms, shown in Figure 6, indicate that for this specific case, even though less propellant is required for PNG than FTVG logic, the integral of acceleration squared, which is chosen as the performance index to derive the optimal logic, has been locally minimized by FTVG logic.

Another advantage of FTVG compared with PNG is that an impact-time constraint can be achieved, as shown in Figure 7. This figure also shows that the shorter the flight time, the less the spacecraft would travel along the initial velocity direction. Thus, by choosing different flight times, the possibility of collision with known obstacles, or a potential surface collision for asteroid soft landing, can be effectively reduced.

Figure 8 shows spacecraft trajectories of Case 2 with the FTVG algorithm. The initial velocity is $\mathbf{v}_0 = (50, 0, 0)$ m/s. Various initial positions, each 2km from the origin, are chosen. The purpose was to verify the relationship between the existence of local minima of performance index and the initial conditions. As demonstrated in Figure 9, when the angle θ is not larger than 30 degrees, there exists a local minimum of the FTVG algorithm as described by Eq. (47).

Case 3: IACG Applied to Asteroid Intercept with Intercept Angle Constraint

The performance of the proposed IACG algorithm is demonstrated by numerical simulations for a variety of initial conditions and desired impact angles. These results are compared with the performance of the PNG algorithm with impact angle constraint.[7]

It is assumed that the spacecraft starts from the initial position $\mathbf{r}_0 = (-1, 0, 0)$ km to hit a desired impact site located at the origin with a given impact angle. In order to evaluate the generality of the proposed IACG logic, various initial angles of θ ranging from 0 to 90 degrees and commanded impact angles λ_f varying from 0 to 90 degrees are simulated. Figure 10 shows the simulation results for Case 3, where both impact-angle and impact-time control requirements have been successfully achieved. It is also shown in Figure 10 that the terminal velocity of the spacecraft controlled by the IACG can become zero when the specified impact angle is 90 degrees. Although this is a somewhat unrealistic situation, it is caused by the nature of an optimal control that minimizes the control effort. As can be seen in Figure 11, the PNG logic fails for certain undesirable initial conditions while the IACG algorithm has no such limitation.

Figure 12 shows further results for Case 3 with an initial velocity of (100, 20, 0) m/s and the required terminal velocity direction $\mathbf{e}_1$ of (1, 0, 0). For this case, we have $v_1 = 100$ m/s and $r_{f1} - r_1 = 1$ km. Using Eq. (53), we obtain $\tau_2 = 30$ s. Depending on the flight time, chosen to be smaller or larger than 30 s, the IACG algorithm results in either a 0-degree or a 180-degree impact angle, as shown in Figure 12. For other situations with initial velocities of $(r_{f1} - r_1)\, v_1 \leq 0$ and $\lambda_f = 0$, the impact angle can be made to be always 0 deg (not 180 deg) for the IACG logic. The right side of Figure 12 shows a comparison of both situations for the specific impact angle control problem.

A further detailed application of these simple feedback guidance laws to a realistic asteroid intercept problem can be found in Ref. 26.

CONCLUSION

In this paper, we have investigated three optimal feedback guidance algorithms that could be applied to planetary or asteroid terminal guidance problems with a variety of terminal constraints. They were: the constrained-terminal-velocity guidance (CTVG), the free-terminal-velocity guidance (FTVG), and the intercept-angle-control guidance (IACG). It was shown that a local minimum solution of an optimal time-to-go exists for a certain set of initial conditions. The proposed IACG concept exploits a simple combination of the FTVG and CTVG algorithms. Numerical simulation results for a few illustrative test cases have indicated that these simple feedback guidance algorithms can be employed to a planetary precision soft landing mission as well as an asteroid intercept problem.

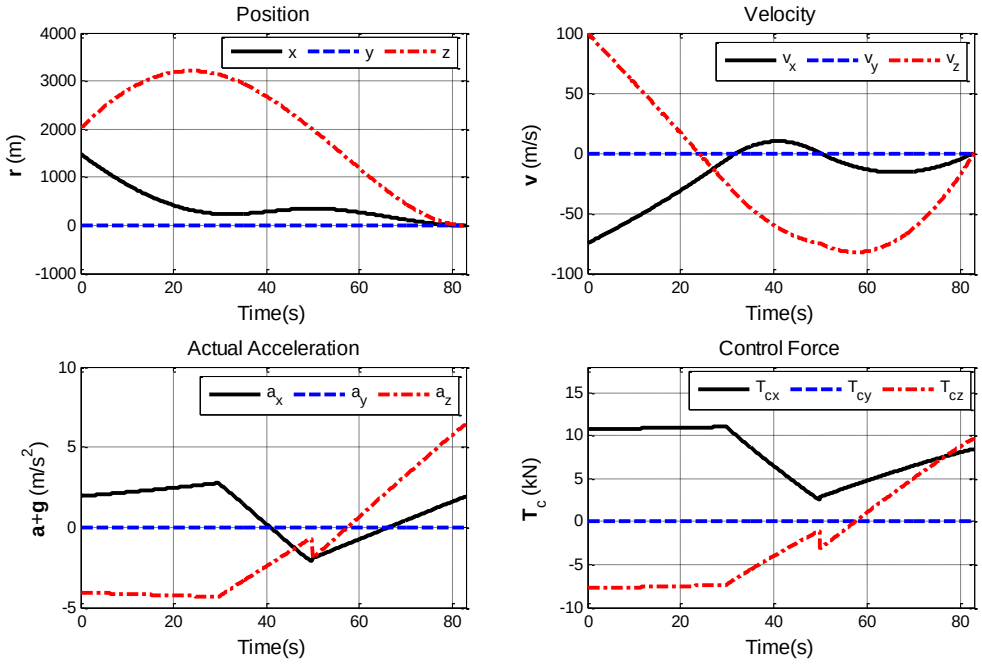

Figure 1. Case 1 with CTVG Algorithm.

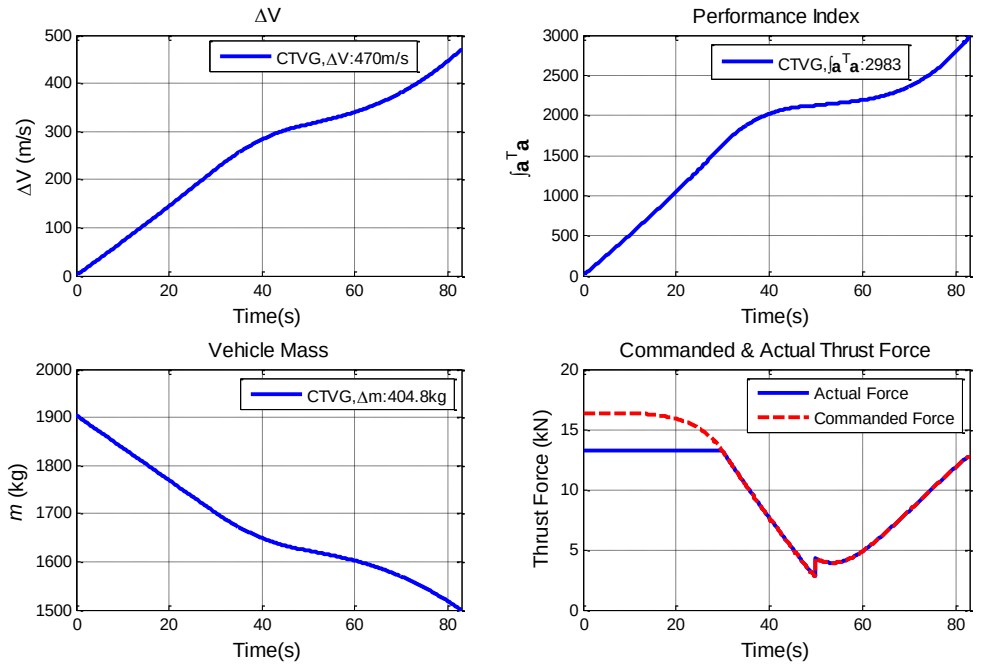

Figure 2. Case 1 with CTVG Algorithm (Continued).

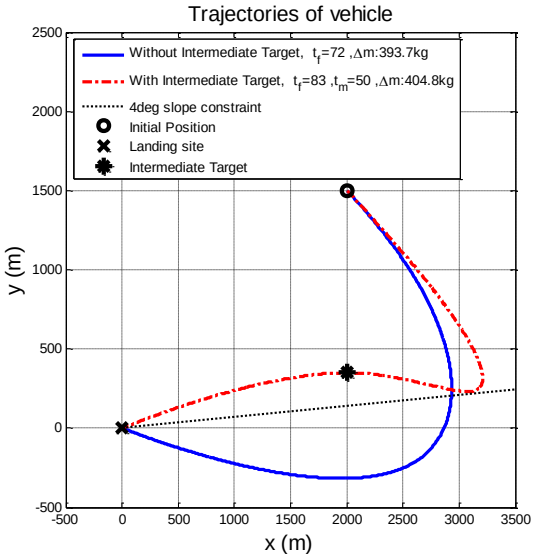

Figure 3. Case 1 with CTVG Algorithm (Continued).

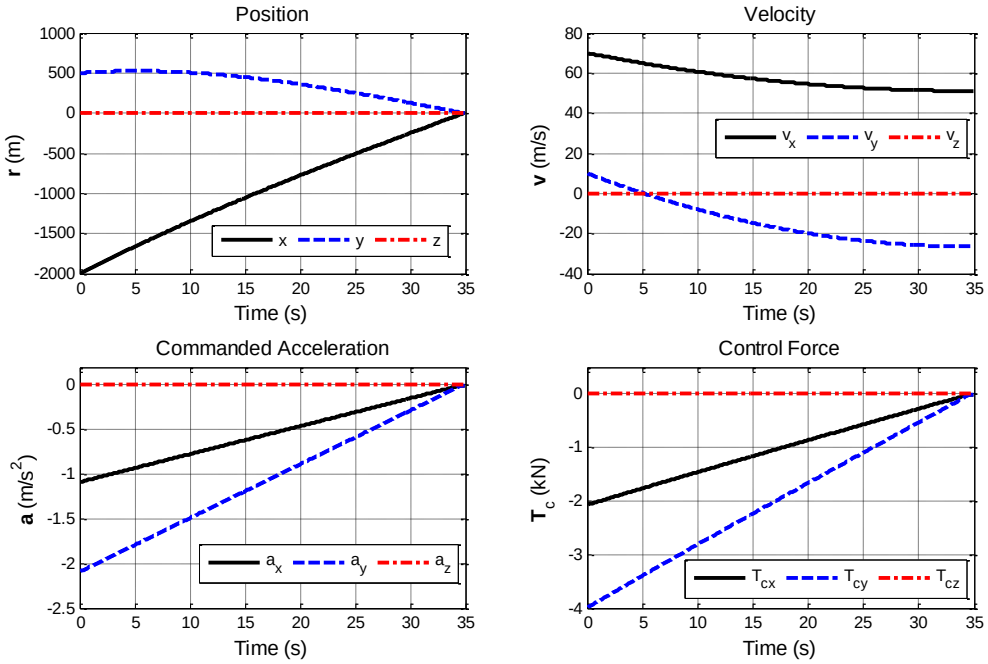

Figure 4. Case 2 with FTVG Algorithm.

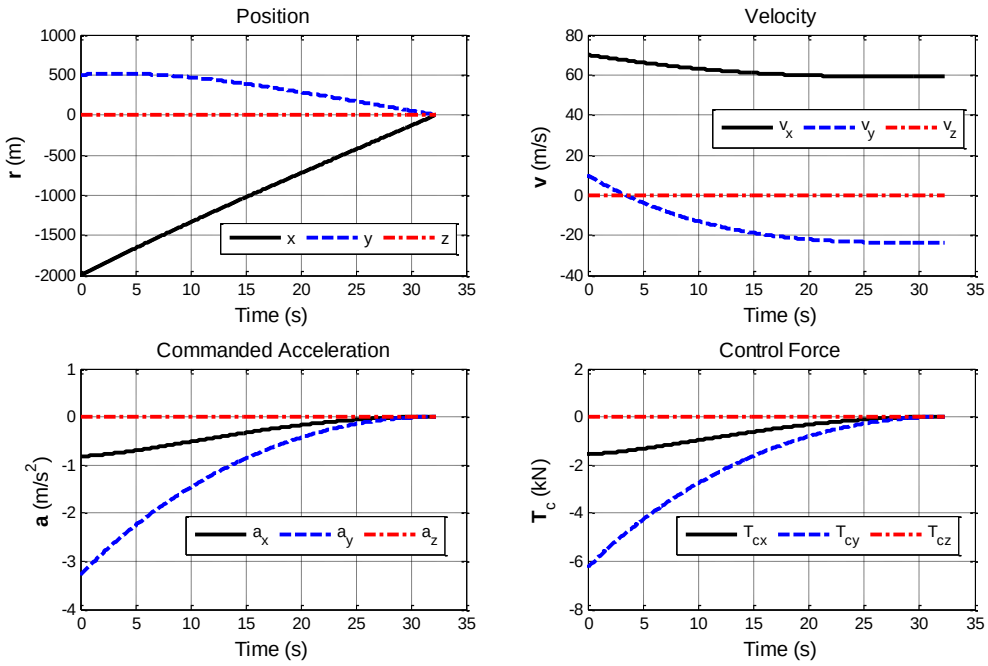

Figure 5. Case 2 with PNG Algorithm.

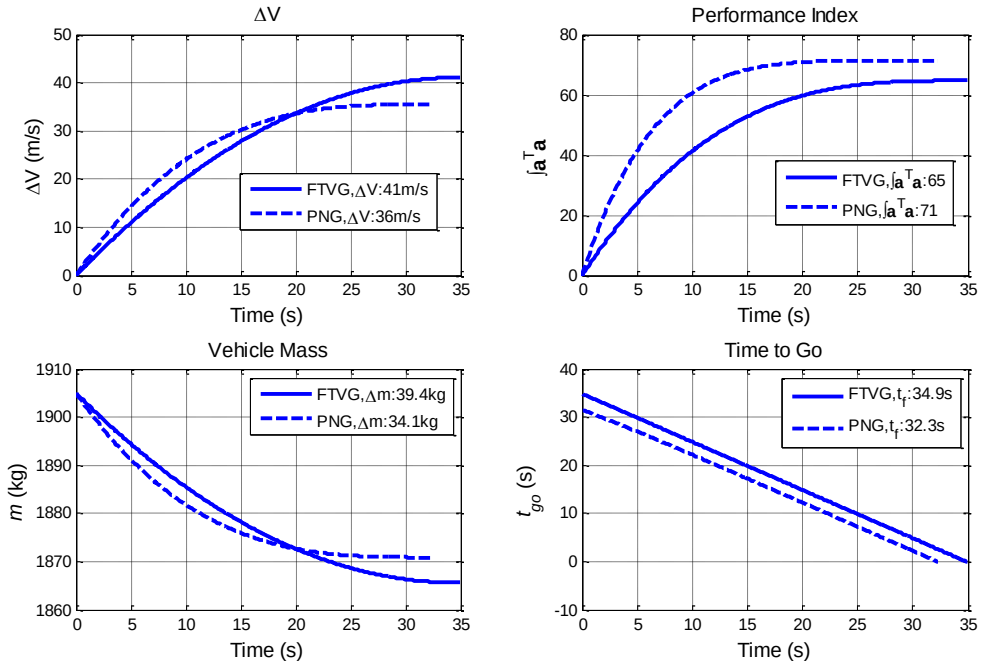

Figure 6. Case 2 with FTVG and PNG Algorithms.

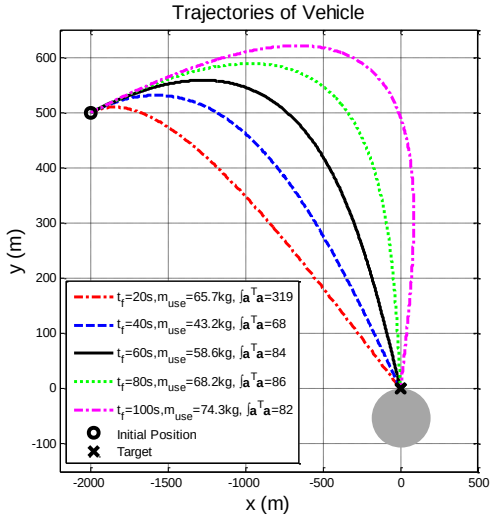

Figure 7. Case 2 with FTVG algorithm for Various Flight Time Requirements.

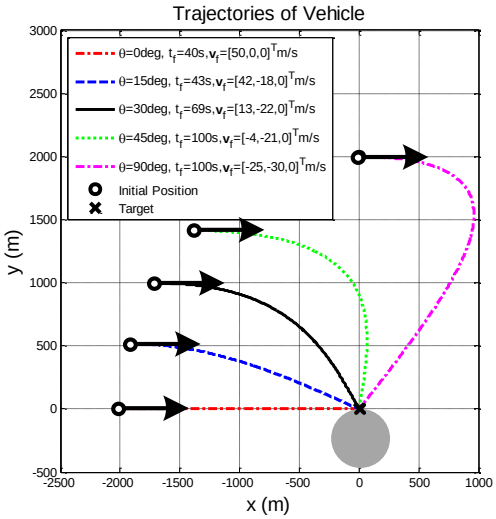

Figure 8. Case 2 with FTVG algorithm for Various Initial Positions.

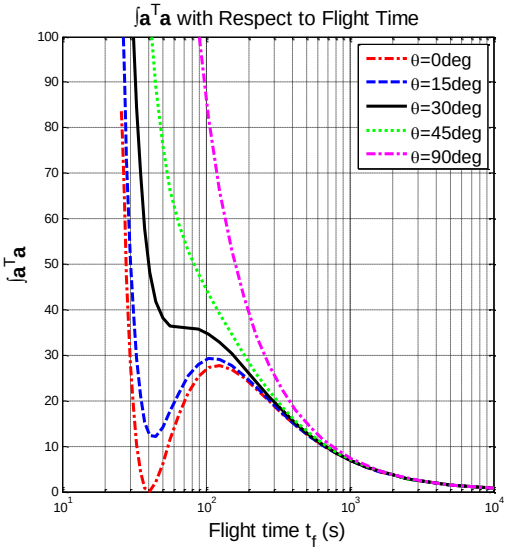

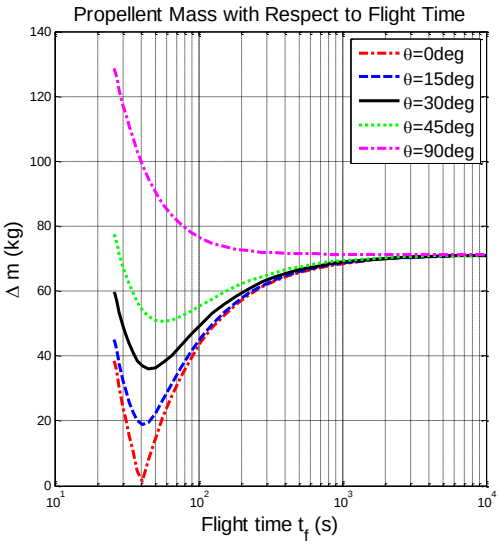

Figure 9. Case 2 with FTVG Algorithm for Various Flight Time Requirements and Different Initial Positions.

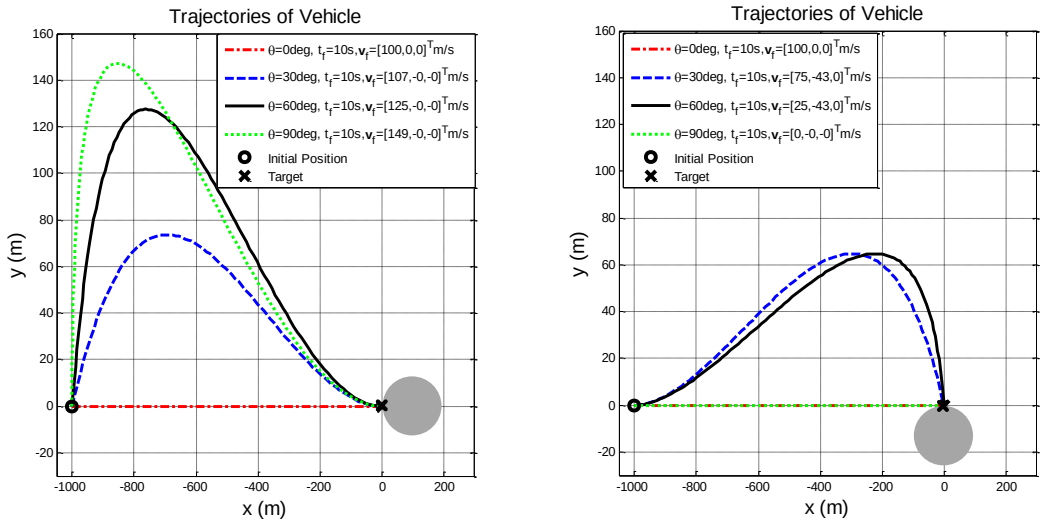

Figure 10. Case 3 with IACG Algorithm for Various Initial Angles and Impact Angle Requirements.

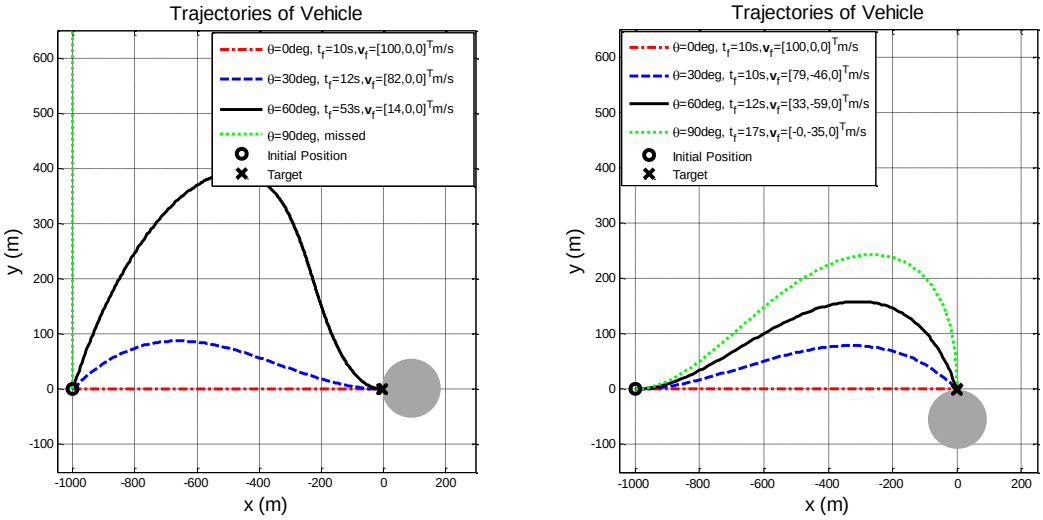

Figure 11. Case 3 for PNG Algorithm with Intercept Angle Constraint for Various Initial Angles and Impact Angle Requirements.

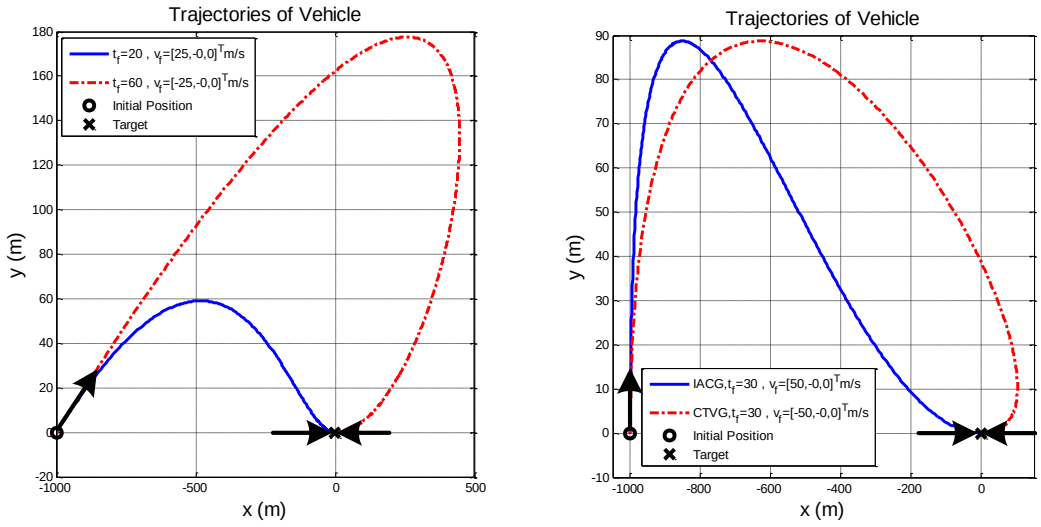

Figure 12. Case 3 with CTVG and IACG algorithms.

ACKNOWLEDGMENTS

This research work was supported by a research grant from the Iowa Space Grant Consortium (ISGC) awarded to the Asteroid Deflection Research Center at Iowa State University. The authors would like to thank Dr. Ramanathan Sugumaran (Director of the ISGC) for his support of this research project.

REFERENCES

[1] C. N. D'Souza, "An Optimal Guidance Law for Planetary Landing," AIAA 1997-3709.

[2] B. Açikmeşe, and S. R. Ploen, "Convex Programming Approach to Powered Descent Guidance for Mars Landing," *Journal of Guidance, Control, and Dynamics*, Vol. 30, No. 5, 2007, pp. 1353-1366.

[3] L. Blackmore, B. Açikmeşe, and D. P. Scharf, "Minimum-Landing-Error Powered-Descent Guidance for Mars Landing Using Convex Optimization," *Journal of Guidance, Control, and Dynamics*, Vol. 33, No. 4, 2010, pp. 1161-1171.

[4] B. A. Steinfeldt, M. J. Grant, D. A. Matz, R. D. Braun and G. H. Barton, "Guidance, Navigation, and Control System Performance Trades for Mars Pinpoint Landing," *Journal of Spacecraft and Rockets*. Vol. 47, No. 1, 2010, pp. 188-198.

[5] A. E. Bryson and Y.-C. Ho, *Applied Optimal Control*, Wiley, New York, 1975, pp. 154-155.

[6] R. H. Battin, *An Introduction to the Mathematics and Methods of Astrodynamics*, AIAA Education Series, AIAA, 1987, pp. 558-561.

[7] P. Zarchan, *Tactical and Strategic Missile Guidance*, Vol. 219, Progress in Astronautics and Aeronautics, 5th ed., AIAA, 2007, pp. 541-547.

[8] B. Ebrahimi, M. Bahrami, and J. Roshanian, "Optimal Sliding-mode Guidance with Terminal Velocity Constraint for Fixed-interval Propulsive Maneuvers," *Acta Astronautiac*, Vol. 62, No. 10-11, 2008, pp. 556-562.

[9] R. Furfaro, S. Selnick, M. L. Cupples, and M. W. Cribb, "Non-Linear Sliding Guidance Algorithms for Precision Lunar Landing," AAS 11-167.

[10] M. Kim and K. V. Grider, "Terminal Guidance for Impact Attitude Angle Constraint Flight Trajectories," *IEEE Transactions on Aerospace and Electronic Systems*, Vol. AES-9, No. 6, November 1973, pp. 269-278.

[11] B. S. Kim, J. G. Lee, and H. S Han, "Biased PNG Law for Impact with Angular Constraint," *IEEE Transactions on Aerospace and Electronic Systems*, Vol. 34, No. 1, January 1998, pp. 277-288.

[12] C. K. Ryoo, H. J. Cho, and M. J. Tahk, "Optimal Guidance Laws with Terminal Impact Angle Constraint," *Journal of Guidance, Control, and Dynamics*, Vol. 28, No. 4, 2005, pp. 724-732.

[13] P. Lu, D. B. Doman, and J. D. Schierman, "Adaptive Terminal Guidance for Hypervelocity Impact in Specified Direction," *Journal of Guidance, Control, and Dynamics*, Vol. 29, No. 2, 2006, pp. 724-732.

[14] V. Shaferman and T. Shima, "Linear Quadratic Guidance Laws for Imposing a Terminal Intercept Angle," *Journal of Guidance, Control, and Dynamics*, Vol. 31, No. 5, 2008, pp. 1400-1412.

[15] A. Ratnoo and D. Ghose, "Impact Angle Constrained Guidance Against Nonstationary Nonmaneuvering Targets," *Journal of Guidance, Control, and Dynamics*, Vol. 33, No. 1, 2010, pp. 269-275.

[16] M. G. Yoon, "Relative Circular Navigation Guidance for Three-Dimensional Impact Angle Control Problem," *Journal of Aerospace Engineering*, Vol. 33, No. 4, 2010, pp. 300-308.

[17] T. Shima, "Intercept-Angle Guidance," *Journal of Guidance, Control, and Dynamics*, Vol. 34, No. 2, 2011, pp. 484-492.

[18] D. Kubitschek, "Impactor Spacecraft Targeting for the Deep Impact Mission to Comet Tempel 1," AAS 03-615.

[19] J. Gil-Fernández, R. Cadenas-Gorgojo, T. Prieto-Llanos, and M. Graziano, "Autonomous GNC Algorithms for Rendezvous Missions to Near-Earth-Objects, " AIAA 2008-7087.

[20] J. Gil-Fernández, R. Panzeca, and C. Corral, "Impacting Small Near Earth Objects," *Advances in Space Research*, Vol. 42, No. 8, October 2008, pp. 1352-1363.

[21] M. Hawkins, A. Pitz, B. Wie, and J. Gil-Fernández, "Terminal-Phase Guidance and Control Analysis of Asteroid Interceptors," AIAA 2010-8348.

[22] M. Hawkins and B. Wie, "Impact-Angle Control of Asteroid Interceptors/Penetrators," AAS 11-271.

[23] H. Seifert (ed.), *Space Technology*, John Wiley, 1959, Chapters 9 and 10.

[24] J. E. Prussing, "Equation for Optimal Power-Limited Spacecraft Trajectories," *Journal of Guidance, Control, and Dynamics*, Vol. 16, No. 2, 1993, pp. 391-393.

[25] B. Conway (ed.), *Spacecraft Trajectory Optimization*, Cambridge University Press, 2010, Chapters 2 and 3.

[26] M. Hawkins, Y. Guo, and B. Wie, "Guidance Algorithms for Asteroid Intercept Missions with Precision Targeting Requirements", AAS 11-531.